PROCEEDINGS OF SCIENCE

Global extraction of unpolarized quark TMDs at N^{3}LL

Alessandro Bacchetta,[a,b] **Valerio Bertone,**[c] **Chiara Bissolotti,**[a,d] **Giuseppe Bozzi,**[e,f,*] **Matteo Cerutti,**[a,b] **Fulvio Piacenza,**[a] **Marco Radici**[b] **and Andrea Signori**[g,h]

[a] *Dipartimento di Fisica, Università di Pavia, via Bassi 6, I-27100 Pavia, Italy*
[b] *INFN - Sezione di Pavia, via Bassi 6, I-27100 Pavia, Italy*
[c] *IRFU, CEA, Université Paris-Saclay, F-91191 Gif-sur-Yvette, France*
[d] *HEP Division, Argonne National Laboratory, 9700 S. Cass Avenue, Lemont, IL, 60439 USA*
[e] *Dipartimento di Fisica, Università di Cagliari, Cittadella Universitaria, I-09042 Monserrato (CA), Italy*
[f] *INFN - Sezione di Cagliari, Cittadella Universitaria, I-09042 Monserrato (CA), Italy*
[g] *Dipartimento di Fisica, Università di Torino, via P. Giuria 1, I-10125 Torino, Italy*
[h] *INFN - Sezione di Torino, via P. Giuria 1, I-10125 Torino, Italy*
E-mail: alessandro.bacchetta@unipv.it, valerio.bertone@cern.ch, chiara.bissolotti01@universitadipavia.it, giuseppe.bozzi@unica.it, matteo.cerutti@pv.infn.it, fu.piacenza@gmail.com, marco.radici@pv.infn.it, andrea.signori@unito.it

We present a recent extraction of unpolarised transverse-momentum-dependent (TMD) parton distribution functions and TMD fragmentation functions from experimental data sets of Semi-Inclusive Deep-Inelastic Scattering, Drell-Yan and Z boson production. The global fit is performed at the N^{3}LL logarithmic accuracy and is based on flexible non-perturbative functions, allowing to reach a very good agreement with data

41st International Conference on High Energy physics - ICHEP2022
6-13 July, 2022
Bologna, Italy

*Speaker

PoS(ICHEP2022)800

1. Introduction

Multi-dimensional maps of the internal structure of the proton are essential ingredients for an increasing understanding of confinement and QCD dynamics. In recent years, the extraction of transverse momentum dependent (TMD) parton distribution functions (PDF) and fragmentation functions (FF) from experimental data has reached a high level of sophistication and we now have global analyses based on both Semi-Inclusive Deep-Inelastic Scattering (SIDIS) and Drell-Yan (DY) data at high perturbative accuracies [1–3].

This contribution is a short summary of results obtained in [1], and we refer the reader to the full publication for all the technical details. The main features of our work can be summarised as follows: we performed a fit of 2031 SIDIS and DY experimental data, at an (approximate) N^{3}LL perturbative accuracy and with a non-perturbative functional form depending on 21 free parameters, obtaining a global $\chi^2/N_{data} = 1.06$.

2. Formalism

In the framework of TMD factorisation [4], the differential cross section for the Drell-Yan process ($h_A h_B \longrightarrow \gamma^*/Z + X \longrightarrow \ell^+\ell^- + X$) can be schematically written in the following form:

$$\frac{d\sigma^{\rm DY}}{dq_T\, dy\, dQ} \propto x_A x_B\, H^{\rm DY}(Q,\mu) \sum_a c_a(Q^2) \int_0^{+\infty} \frac{db_T}{2\pi} b_T J_0\big(b_T q_T\big) \hat{f}_1^a(x_A, b_T^2; \mu, \zeta_A)\, \hat{f}_1^{\bar{a}}(x_B, b_T^2; \mu, \zeta_B) \tag{1}$$

where q_T, y and Q are the transverse-momentum, rapidity and invariant mass of the lepton pair, respectively. The hard factor H^{DY} admits a perturbative expansion, is equal to 1 at leading order and depends on the renormalisation scale μ. The Q-dependent c_a's are the electroweak charges of the quarks. The unpolarised quark TMD parton distribution functions $\hat{f}_1^a$ and $\hat{f}_1^{\bar{a}}$ depend on the longitudinal momentum fractions x_A, x_B, on the Fourier-conjugate variable b_T to the (non-measured) quark transverse-momentum $k_\perp$, and on the renormalisation(μ) and rapidity(ζ) scales.

A similar schematic form for the differential cross section for the SIDIS process ($\ell N \longrightarrow \ell h + X$) reads as follows:

$$\frac{d\sigma^{\rm SIDIS}}{dx\, dz\, dq_T\, dQ} \propto x\, H^{\rm SIDIS}(Q,\mu) \sum_a e_a^2 \int_0^{+\infty} \frac{db_T}{2\pi} b_T J_0\big(b_T q_T\big) \hat{f}_1^a(x, b_T^2; \mu, \zeta_A)\, \hat{D}_1^{a\to h}(z, b_T^2; \mu, \zeta_B) \tag{2}$$

where x, z, q_T, Q are the standard kinematic SIDIS variables, q_T and Q being the photon transverse-momentum and the four-momentum transfer, respectively. The hard factor H^{SIDIS} can again be calculated order by order in perturbation theory, and we have introduced the unpolarised quark TMD fragmentation function $D_1^{a\to h}$. In this case, b_T is the Fourier-conjugate variable to q_T which, at low transverse-momenta, is related to the measured hadron P_{hT} through the formula: $q_T \approx -P_{hT}/z \approx -(k_\perp + P_\perp/z)$, where $P_\perp$ is the (non-measured) transverse momentum of the hadron relative to the quark.

The general structure of a TMD parton distribution function is

$$\hat{f}_1^a(x, b_T^2; \mu_f, \zeta_f) = [C \otimes f_1](x, b_*; \mu_{b_*}, \mu_{b_*}^2) \exp\left\{ \int_{\mu_{b_*}}^{\mu_f} \frac{d\mu}{\mu} \gamma\big(\mu, \zeta_f\big) \right\} \left(\frac{\zeta_f}{\mu_{b_*}^2} \right)^{K(b_*, \mu_{b_*})/2} f_1^{NP}(x, b_T^2) \tag{3}$$

The coefficient function C provides the matching to collinear PDFs f_1 in the small b_T region ($b_T \ll 1/\Lambda_{QCD}$) and is computable order by order in perturbation theory. The γ and K functions are the anomalous dimension and the Collins-Soper, respectively, dictating the evolution of the TMD up to large b_T values. They also admit a perturbative expansion. The b_T variable is replaced by a b_* which saturates at a fixed b_{max}: this guarantees that the scale $\mu_{b_*} = 2e^{-\gamma_E}/b_*$ is sufficiently larger than the QCD Landau pole and, thus, that the TMD is perturbatively meaningful. The perturbative order at which the above quantities are included in the theoretical predictions determine the accuracy of the fit: in our case, H and C are computed at the second order, K at the third order and γ at the fourth order in the strong coupling, allowing us to reach the N^{3}LL accuracy. Collinear PDFs and FFs should also be included at the corresponding accuracy. However, when we performed the fit, collinear PDFs were available at NNLO while collinear FFs were not and we included them at NLO. For this reason we dubbed "N^{3}LL$^-$" the perturbative accuracy of our fit.

The f_1^{NP} factor[1] is the genuine non-perturbative contribution that we fit from experimental data. Its functional form is largely arbitrary, though based on model calculations of TMD PDFs and FFs, and is chosen in such a way that $f_1^{NP} \to 1$ and $D_1^{NP} \to 1$ in the $b_T \to 0$ limit.
For the TMD PDF we define

$$f_1^{NP}(x, b_T^2) = \frac{g_1(x)\, e^{-g_1(x)\frac{b_T^2}{4}} + \lambda^2\, g_{1B}^2(x) \left[1 - g_{1B}(x)\frac{b_T^2}{4}\right] e^{-g_{1B}(x)\frac{b_T^2}{4}} + \lambda_2^2\, g_{1C}(x)\, e^{-g_{1C}(x)\frac{b_T^2}{4}}}{g_1(x) + \lambda^2\, g_{1B}^2(x) + \lambda_2^2\, g_{1C}(x)}\,. \tag{4}$$

For the analogous D_1^{NP} factor in the TMD FF, entering the SIDIS formula, we define

$$D_1^{NP}(z, b_T^2) = \frac{g_3(z)\, e^{-g_3(z)\frac{b_T^2}{4z^2}} + \frac{\lambda_F}{z^2}\, g_{3B}^2(z) \left[1 - g_{3B}(z)\frac{b_T^2}{4z^2}\right] e^{-g_{3B}(z)\frac{b_T^2}{4z^2}}}{g_3(z) + \frac{\lambda_F}{z^2}\, g_{3B}^2(z)}\,. \tag{5}$$

The g_i functions describe the dependence of the widths of the distributions on x and z:

$$g_{\{1,1B,1C\}}(x) = N_{\{1,1B,1C\}} \frac{x^{\sigma_{\{1,2,3\}}}(1-x)^{\alpha^2_{\{1,2,3\}}}}{\hat{x}^{\sigma_{\{1,2,3\}}}(1-\hat{x})^{\alpha^2_{\{1,2,3\}}}}\,, \tag{6}$$

$$g_{\{3,3B\}}(z) = N_{\{3,3B\}} \frac{(z^{\beta_{\{1,2\}}} + \delta^2_{\{1,2\}})(1-z)^{\gamma^2_{\{1,2\}}}}{(\hat{z}^{\beta_{\{1,2\}}} + \delta^2_{\{1,2\}})(1-\hat{z})^{\gamma^2_{\{1,2\}}}}\,, \tag{7}$$

where $\hat{x} = 0.1$, $\hat{z} = 0.5$. We have, in total, 21 free parameters to fit: one from the non-perturbative part of the Collins-Soper kernel K (see the previous footnote), 11 for the TMD PDF and 9 for the TMD FF.

When comparing theoretical predictions with experimental SIDIS data, we observe a good agreement at NLL accuracy but a severe underestimation of N^{2}LL and N^{3}LL perturbative results with respect to both HERMES and COMPASS data. The suppression of theoretical predictions is

[1] In order to improve readability, here we write a simplified version of the non-perturbative form factor, i.e., we omit the non-perturbative correction term to the Collins-Soper kernel: a factor $\left[\frac{\zeta}{Q_0^2}\right]^{g_K(b_T^2)/2}$ should be appended both to f_1^{NP} and D_1^{NP}.

largely due to the inclusion of higher orders in the H function in Eq.(2). An extensive discussion on this topic can be found in [5]. This led us to the introduction of a normalisation pre-factor, chosen in such a way to correctly recover the integrated (DIS) cross-section. We stress that these multiplicative factors only depend on the collinear PDFs and FFs, are computed before performing the fit and are totally independent on the functional form of the non-perturbative contribution.

3. Data

Since the TMD formalism is only valid in the small-q_T region, we choose to impose the following cuts on experimental data:

$$q_T < 0.2\,Q \quad \text{(DY)} \qquad |P_{hT}| < \min\Big[\,\min[c_1\,Q, c_2\,zQ] + c_3\,\text{GeV},\; zQ\Big] \quad \text{(SIDIS)} \tag{8}$$

with fixed parameters $c_1 = 0.2$, $c_2 = 0.5$ and $c_3 = 0.3$. The number of points passing the cuts is 484 for the Drell-Yan process, coming from Fermilab fixed-target experiments, STAR, PHENIX, Tevatron (CDF and D0 at Run I and Run II) and LHC (ATLAS, CMS, LHCb at 7,8,13 TeV). As for the SIDIS process, the flexibility of the z-dependent formula in Eq.(8) allowed us to include 1547 data points from the HERMES and COMPASS datasets. Our global analysis, thus, rely on a total number of 2031 data points, whose coverage in x vs. Q^2 is shown in Fig.1.

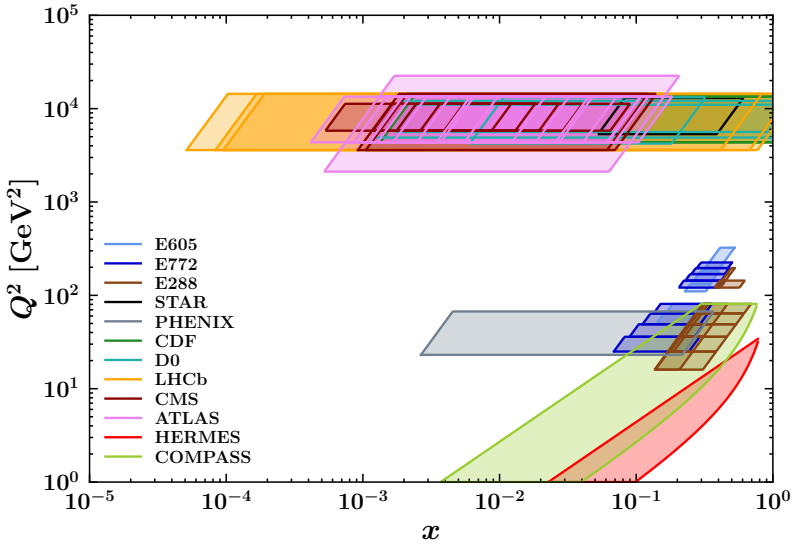

Figure 1: The $x - Q^2$ coverage of the experimental data used for the fit.

4. Results

The quality of the fit is represented by the χ^2 value of the best fit to the experimental data: $\chi^2_0 = 1.06$. This result shows that we are able to simultaneously describe data from two different processes over a wide kinematic range. The error analysis is based on the so-called bootstrap

method, i.e. the fitting of Monte Carlo replicas (250, in our case) of the datasets and the subsequent derivation of uncertainties from confidence level intervals.

After the introduction of the normalisation factor, the agreement with SIDIS data is particularly satisfactory for each dataset. As for the DY case, we observe some discrepancy with ATLAS data that might be due to theoretical corrections not included in the present analysis but relevant when comparing to very high precision data.

In the upper plots of Fig.(2) we show the TMD PDF for the up quark at $Q = 2$ GeV and $Q = 10$ GeV as a function of the quark transverse momentum $k_\perp$ for $x = 0.001, 0.01, 0.1$. The uncertainty bands correspond to the envelope of 68% of the replicas generated with the bootstrap method. We notice that at $x = 0.01$ the TMD seems more widespread, while at $x = 0.001$ its tail extends well above 1 GeV for $Q = 10$ GeV. The $x = 0.001$ TMD has also the largest error band (at low $k_\perp$, in particular) mainly because of the very few data points in this kinematic region.

In the lower plots of Fig.(2) we show the unpolarised TMD FF for an up quark fragmenting into a π^+ at $Q = 2$ GeV and $Q = 10$ GeV as a function of the hadron transverse momentum $|P_\perp|$ for $z = 0.3$ and 0.6. In addition to the high tails, we notice the emergence of a structure at intermediate $P_\perp$ that deserves further studies and would benefit from electron-positron annihilation data for better interpretation. Possible extensions of this work include the introduction of theoretical uncertainties via suitable scale variations (along the lines of [6]) and the investigation of flavour-dependent effects [7, 8].

The complete list of results obtained from the fit presented in this contribution will be available in a public git repository [9].

Acknowledgments

This work is supported by the European Union's Horizon 2020 programme under grant agreement No. 824093 (STRONG2020). The authors warmly thank the organizers of ICHEP 2022 for putting up a very stimulating conference and for allowing us to present these results.

References

[1] A. Bacchetta, V. Bertone, C. Bissolotti, G. Bozzi, F. Delcarro, F. Piacenza and M. Radici, *Transverse-momentum-dependent parton distributions up to N^{3}LL from Drell-Yan data, JHEP* **07** (2020), 117 [arXiv:1912.07550 [hep-ph]].

[2] A. Bacchetta, F. Delcarro, C. Pisano, M. Radici and A. Signori, *Extraction of partonic transverse momentum distributions from semi-inclusive deep-inelastic scattering, Drell-Yan and Z-boson production, JHEP* **06** (2017), 081 [erratum: JHEP **06** (2019), 051] [arXiv:1703.10157 [hep-ph]].

[3] I. Scimemi and A. Vladimirov, *Non-perturbative structure of semi-inclusive deep-inelastic and Drell-Yan scattering at small transverse momentum, JHEP* **06** (2020), 137 [arXiv:1912.06532 [hep-ph]].

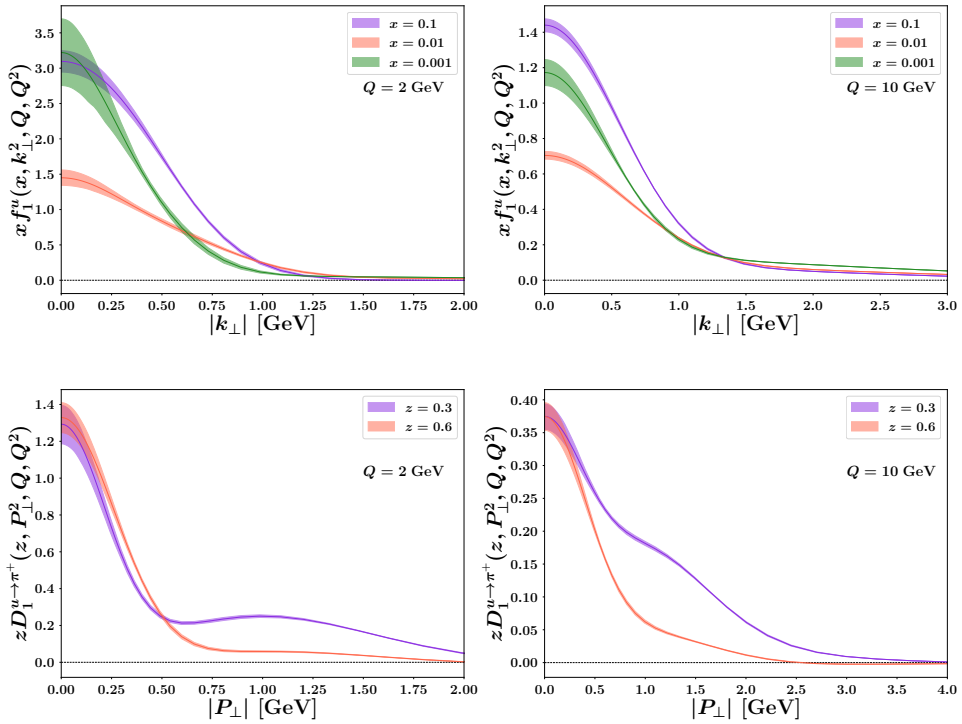

Figure 2: *Upper plots:* the TMD PDF of the up quark in a proton at $Q = 2$ GeV (left panel) and 10 GeV (right panel) as a function of the partonic transverse momentum $|k_\perp|$ for $x = 0.001$, 0.01 and 0.1.
Lower plots: the TMD FF for an up quark fragmenting into a π^+ at $Q = 2$ GeV (left panel) and 10 GeV (right panel) as a function of the hadron transverse momentum $|P_\perp|$ for $z = 0.3$ and 0.6.
The uncertainty bands in all plots represent the 68%CL.

[4] J. Collins, *Foundations of perturbative QCD, Camb. Monogr. Part. Phys. Nucl. Phys. Cosmol.* **32** (2011), 1-624 Cambridge University Press, 2013, ISBN 978-1-107-64525-7, 978-1-107-64525-7, 978-0-521-85533-4, 978-1-139-09782-6

[5] F. Piacenza, *Perturbative and nonperturbative QCD regimes in transverse-momentum dependent observables, PhD Thesis*: University of Pavia (2020)

[6] V. Bertone, G. Bozzi and F. Hautmann, *Perturbative hysteresis and emergent resummation scales, Phys. Rev. D* **105** (2022) no.9, 096003 [arXiv:2202.03380 [hep-ph]].

[7] A. Bacchetta, G. Bozzi, M. Radici, M. Ritzmann and A. Signori, *Effect of Flavor-Dependent Partonic Transverse Momentum on the Determination of the W Boson Mass in Hadronic Collisions, Phys. Lett. B* **788** (2019), 542-545 [arXiv:1807.02101 [hep-ph]].

[8] G. Bozzi and A. Signori, *Nonperturbative Uncertainties on the Transverse Momentum Distribution of Electroweak Bosons and on the Determination of the Boson Mass at the LHC, Adv. High Energy Phys.* **2019** (2019), 2526897 [arXiv:1901.01162 [hep-ph]].

[9] https://github.com/MapCollaboration/NangaParbat